Gas Separation Hot Paper

International Edition: DOI: 10.1002/anie.202000029
German Edition: DOI: 10.1002/ange.202000029

Enhanced Propene/Propane Separation by Directional Decoration of the 12-Membered Rings of Mordenite with ZIF Fragments

Yaqi Wu[+], Shu Zeng[+], Danhua Yuan, Jiacheng Xing, Hanbang Liu, Shutao Xu, Yingxu Wei, Yunpeng Xu, and Zhongmin Liu**

Abstract: *Propene/propane separation is challenging due to the very small difference in molecular sizes, boiling points and condensabilities between these molecules. Herein, we report a strategy of introducing ZIF fragments into traditional mordenite (MOR) zeolite to decorate the 12-membered ring of MOR. After decoration, the originally ineffective zeolite MOR exhibited high kinetic propene/propane selectivities (139 at 25 °C) and achieved efficient propene/propane separation. The propene/propane separation potentials of the resulting adsorbents were further confirmed by breakthrough experiments with equimolar propene/propane (50/50) mixtures.*

Olefin/paraffin separation is believed to be one of seven chemical separations that will change the world.[1] The very similar physical and chemical properties of propene and propane make the currently used cryogenic distillation highly energy-consuming and expensive.[2] Adsorption separation is thought to be a promising alternative with lower energy consumption and cost. Nevertheless, the development of adsorbents for efficient propane/propene separation remains challenging in the gas separation field. Due to their tunable porosities and adjustable surface group functionalities, several MOFs exhibit kinetic separation performance towards propene and propane.[3] Traditional zeolites are one of the most important classes of porous materials featuring easy synthesis, low cost and high stability. It has been recognized that Lewis or Brönsted acid sites inside the zeolite framework can cause strong adsorption of propene and may catalyze the polymerization of propene inside the pores.[3c] With well-defined structures, very few 8-memberd ring silicate zeolites show potential for the kinetic separation of propene/propane, and the synthetic processes of these materials are relatively difficult.[4]

In our recent work, the strategy of decorating traditional zeolites with MOF subunits proved to be efficient for increasing the CH_4/N_2 selectivities of zeolites.[5] Here, we developed a series of propene/propane adsorbents by decorating mordenite (MOR) with ZIF fragments whose significant kinetic selectivities were determined. The 12-membered ring (12-MR) of MOR was directionally decorated by ZIF fragments, which were anchored the imidazoles inside the zeolite pores by taking advantage of the strong covalent binding between Zn^{2+} and imidazole groups. The introduction of the three different fragments resulted in different degrees of 12-MR decoration, and the diffusion of propene and propane molecules was greatly affected; the adsorption amount of propene remained constant or even slightly increased, whereas the adsorption amount of propane decreased dramatically. Thus, the originally ineffective MOR showed good separation performance towards propene/propane. Moreover, the acid sites of MOR were occupied upon decoration, and the strong adsorption of propene by MOR was also significantly eliminated. Three different fragments, ZIF-8 fragments (Zn-mIM, mIM = 2-methylimidazole), ZIF-14 fragments (Zn-eIM, eIM = 2-ethylimidazole) and their derivatives Zn-pIM (pIM = 2-propylimidazole), were used. Typically, cation-exchange occurred first to convert the zeolite MOR to zinc form, which then reacted with mIM (decorated with Zn-mIM), and the product was denoted ZnMOR-mIM (for details, see the Supporting Information). The proposed process and typical structures of the adsorbents are illustrated in Scheme 1.

The ICP-OES results indicated that MOR underwent successful cation-exchange to form ZnMOR (Table S1). Characteristic resonances of mIM^-, eIM^- and pIM^- were

[*] Y. Wu,[+] S. Zeng,[+] Dr. D. Yuan, J. Xing, H. Liu, Prof. Dr. S. Xu, Prof. Dr. Y. Wei, Prof. Dr. Y. Xu, Prof. Dr. Z. Liu
National Engineering Laboratory for Methanol to Olefins, Dalian National Laboratory for Clean Energy, Dalian Institute of Chemical Physics, Chinese Academy of Sciences
Dalian 116023 (P. R. China)
E-mail: xuyp@dicp.ac.cn
liuzm@dicp.ac.cn
Y. Wu,[+] S. Zeng,[+] J. Xing, H. Liu
University of Chinese Academy of Sciences
Beijing 100049 (P. R. China)
[+] These authors contributed equally to this work.
Supporting information and the ORCID identification number(s) for the author(s) of this article can be found under https://doi.org/10.1002/anie.202000029.

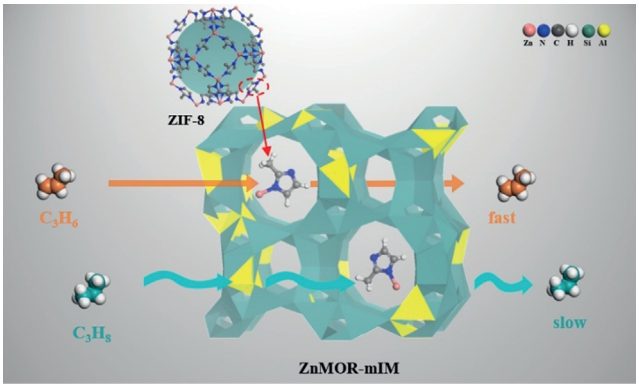

Scheme 1. Schematic illustration of the propene and propane adsorption process on MOR decorated with ZIF-8 fragments.

observed in the ^{13}C CP/MAS NMR spectra (Figure S2).[6] Zn 2p XPS spectra revealed that compared with pristine ZnMOR, the binding energy for Zn 2p in decorated MOR shifted toward lower values and tended to close to that of ZIF-8, suggesting the bonding of Zn^{2+} and imidazolate ions in decorated MOR zeolites and the formation of Zn-IM fragments (Figure S3). ^{15}N CP/MAS NMR spectra also indicated the formation of ZIF fragments (Figure S4). Compared with the Brunauer-Emmett-Teller (BET) surface areas (S_{BET}) and micropore surface areas (S_{micro}) of pristine MOR, those of ZnMOR-mIM, ZnMOR-eIM and ZnMOR-pIM decreased dramatically as a function of Zn-IM decoration (Table S1). The significant decreases in the S_{BET} and S_{micro} of MOR suggested that the Zn-IM fragments occupied the space inside the MOR pores. TGA revealed (Figure S5) that the combination of imidazoles and zeolite were very stable, and the imidazoles were not lost until approximately 500 °C, which also confirmed the covalent binding of Zn^{2+} and imidazolate ions. PXRD patterns (Figure S6) of the resulting adsorbents indicated that the crystalline structure of MOR remained intact after decoration of ZIF fragments. SEM images (Figure S7) also revealed that there were no obvious changes in the morphology between pristine MOR and the decorated MOR.

Single-component adsorption isotherms of propene and propane on pristine and decorated MOR are presented in Figure S8. Before decoration, the pristine zeolite HMOR and ZnMOR exhibited similar adsorption amounts of propene and propane. After decoration, the adsorption amounts of propene remained the same or even slightly increased, while the adsorption amounts of propane decreased dramatically, from 1.14 mmol g^{-1} of ZnMOR to 0.50 mmol g^{-1}, 0.54 mmol g^{-1} and 0.58 mmol g^{-1} of ZnMOR-mIM, ZnMOR-eIM and ZnMOR-pIM, respectively, at 25 °C and 100 kPa. Moreover, for comparison, HMOR-eIM was prepared by direct reaction of 2-eIM with HMOR, and both the propene and propane uptake decreased to a large extent, confirming the unique superiority of decoration with ZIF fragments (Zn-IMs).

Time-dependent propene and propane kinetic adsorptions of pristine and decorated MOR were measured at 25 °C and 50 kPa (Figure 1). NaMOR, HMOR (Figure S9) and ZnMOR did not exhibit large differences in the kinetic adsorption of propene and propane. Upon decoration with ZIF fragments, the diffusion of propane inside the zeolite was affected significantly, with considerably faster uptake of propene over propane. Furthermore, the diffusion time constants D/r^2 were calculated from the kinetic adsorption profiles and kinetic selectivities were obtained as the ratio of the diffusion time constants of propene and propane (Table 1).[3b,7] For the pristine MOR, the propene diffusion rate was slightly lower than that of propane, which may be due to the stronger adsorption interaction of propene with MOR. After decoration, the accessible strong adsorption sites decreased to a large extent, and the larger propane molecule was affected more than propene by the large ZIF fragments, resulting in an obvious decrease in diffusion rates. Therefore, the kinetic selectivities of the decorated MOR adsorbents greatly improved, and ZnMOR-mIM, ZnMOR-eIM and ZnMOR-pIM achieved high kinetic selectivity of 75, 118 and 139, respectively.

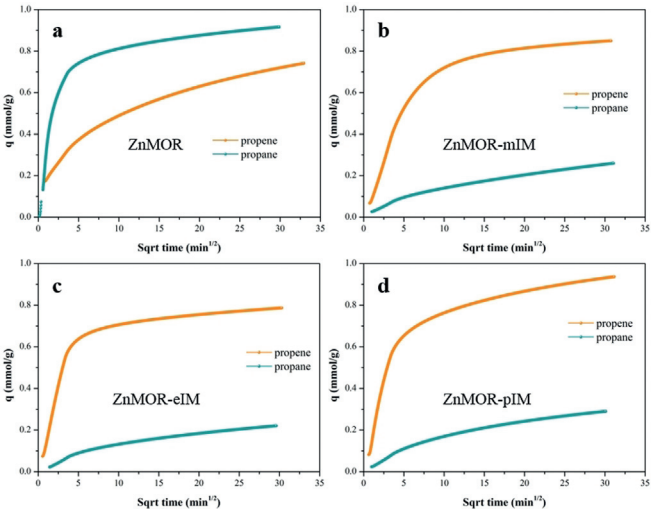

Figure 1. Time-dependent propene and propane uptake profiles for a) ZnMOR, b) ZnMOR-mIM, c) ZnMOR-eIM and d) ZnMOR-pIM at 50 kPa and 25 °C.

Table 1: Kinetic selectivities for the uptake of propene over propane in NaMOR, HMOR, ZnMOR, ZnMOR-mIM, ZnMOR-eIM and ZnMOR-pIM, expressed as the ratio of the two relevant diffusion time constants (D/r^2).

Sample	Diffusion time constant D/r^2 (s^{-1}) Propene	Propane	Kinetic selectivity
NaMOR	7.67×10^{-4}	4.03×10^{-4}	1.90
HMOR	6.12×10^{-6}	4.61×10^{-5}	0.13
ZnMOR	3.50×10^{-6}	3.40×10^{-5}	0.10
ZnMOR-mIM	1.71×10^{-5}	2.27×10^{-7}	75
ZnMOR-eIM	2.01×10^{-5}	1.70×10^{-7}	118
ZnMOR-pIM	1.98×10^{-5}	1.42×10^{-7}	139

The propene/propane separation potential of the resulting adsorbents was further verified by breakthrough experiments with binary mixtures of equimolar propene/propane (50:50). Breakthrough curves of the resulting samples are shown in Figure 2. The pristine zeolite ZnMOR exhibited almost no propene/propane separation performance, for which propene and propane eluted from the packed bed at almost the same time and the separation factor $\alpha_{propene/propane}$ is 1.0. For the decorated ZnMOR-mIM, ZnMOR-eIM and ZnMOR-pIM adsorbents, propane achieved a fast breakthrough at approximately 3 min, which were equivalent to 0.06 mmol g^{-1}, 0.08 mmol g^{-1} and 0.09 mmol g^{-1} uptakes for ZnMOR-mIM, ZnMOR-eIM and ZnMOR-pIM, respectively. Whereas propene was retained in the packed bed until 9–14 min, which were equivalent to 0.31 mmol g^{-1}, 0.47 mmol g^{-1} and 0.53 mmol g^{-1} uptakes for ZnMOR-mIM, ZnMOR-eIM and ZnMOR-pIM, respectively. The separation factors $\alpha_{propene/propane}$ were 5.2, 5.9 and 5.9 for ZnMOR-mIM, ZnMOR-eIM and ZnMOR-pIM, respectively. The breakthrough adsorption amounts of propene and propane were lower than the adsorption amounts from single component isotherms. Because for those decorated MOR, kinetic component plays

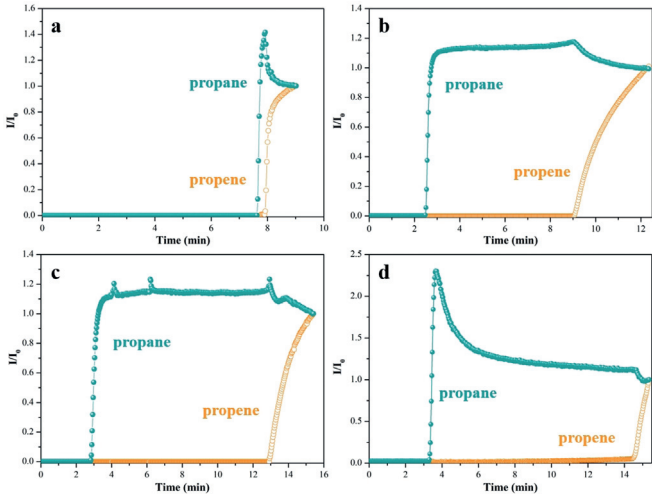

Figure 2. Breakthrough curves of equimolar propane/propene (50:50, v/v) mixtures on a) ZnMOR, b) ZnMOR-mIM, c) ZnMOR-eIM and d) ZnMOR-pIM at 25 °C and 100 kPa.

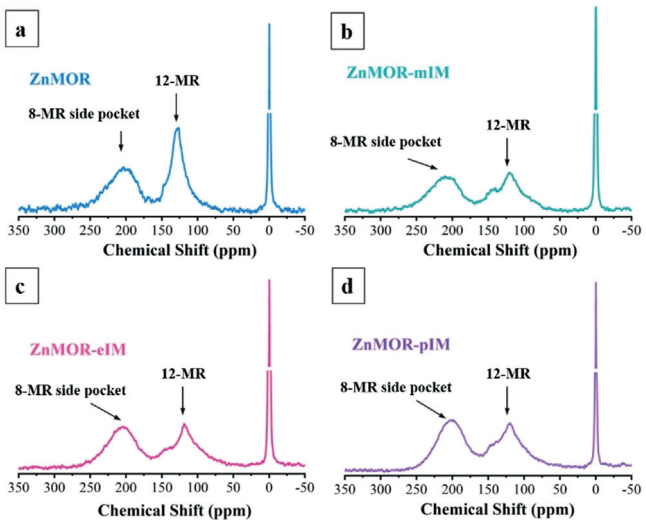

Figure 3. HP-^{129}Xe NMR of a) ZnMOR, b) ZnMOR-mIM, c) ZnMOR-eIM and d) ZnMOR-pIM at −60 °C (0 ppm: Xe in the gas phase).

a significant role in the dynamic separation processes. The breakthrough time of propene and propane were far less than the equilibrium time of adsorption. It also indicated that propene/propane separation performance of decorated adsorbents were mainly influenced by kinetic factors. Breakthrough cycle experiments revealed that after the first cycle and regeneration under vacuum (2 kPa, 25 °C, 2 h), the breakthrough time of both propene and propane on pristine ZnMOR decreased to a large extent and could not be recovered due to the strong adsorption effect (Figure S10). Nevertheless, upon regeneration under vacuum (2 kPa, 25 °C, 2 h), there were slight decreases in the uptakes of propene and propane on decorated ZnMOR-mIM and ZnMOR-eIM, which retained their highly efficient propene/propane separation performance, and exhibited good reproducibility after the first breakthrough experiment. While for ZnMOR-pIM, due to the larger size of Zn-pIM fragments, less strong adsorption sites were occupied and the reproducibility was poorer than that of ZnMOR-mIM and ZnMOR-eIM (Figure S10).

The above results indicated that the strategy of decorating MOR with ZIF fragments is clearly successful, which converts the futile zeolite HMOR and ZnMOR into highly efficient adsorbents for propene/propene separation. Further characterizations were carried out to determine the reason for this interesting phenomenon. Figure 3 shows the HP-^{129}Xe NMR results of the resulting adsorbents. In the HP-^{129}Xe NMR spectra, two distinct resonances except for 0 ppm which assigned to free gas xenon were observed for zeolite MOR, which was similar to the previously reported literature.[8] The resonance at low fields could be ascribed to Xe adsorbed in the 8-membered ring (8-MR) side pocket, and the resonance at high fields could be assigned to Xe in the 12-membered ring (12-MR).[8] The broadening linewidth of the peak attributed to Xe in the 12-MR indicated the decreased mobility of Xe in the12-MR, while that of the peak attributed to Xe in the 8-MR side pocket was almost unchanged.[9] After decoration, the peak attributed to Xe in the 12-MR of the decorated adsorbents was relatively decreased compared to the peak attributed to Xe in the 8-MR side pocket, suggesting that the decoration strategy primarily resulted in decoration of the 12-MR and the 8-MR side pockets were hardly decorated due to the large size of the Zn-IM fragments. That is, the 12-MR of MOR has been directionally decorated, and the 8-MR side pockets were less affected, which was similar to previous reports.[8b,10] The pore size distributions calculated by density functional theory (DFT) based on the Ar adsorption isotherms also confirmed this conclusion (Figure S11). It may also be inferred that the 12-MR of MOR near the pore mouth were decorated. As many studies have reported, some 8-MR zeolites exhibited good kinetic propene/propane separation performances.[4] Moreover, guest gas molecules can only enter the 8-MR side pockets through the 12-MR.[8b] Therefore, it is not difficult for us to understand that after decoration, ZnMOR-mIM, ZnMOR-eIM and ZnMOR-pIM exhibited high kinetic propene/propane selectivities: the diffusion of propane decreased to a large extent, while the diffusion of propene increased due to the decreases in the number of acid sites occupied by imidazole decoration. The resulting adsorbents also exhibited comparable kinetic selectivities to the current typical MOFs (Table S2), which certifies the effectiveness and potential of the strategy of decorating traditional zeolite with ZIF fragments. In-situ Fourier transform infrared spectroscopy using pyridine as a probe molecule (Py-FTIR) also demonstrated the substantial decreases in the number of acid sites in the 12-MR of MOR (Figure S12). The simple decoration strategy with ZIF fragments resulted in highly efficient propene/propane separation performances of the originally ineffectual MOR, reflecting the perfect combination of traditional zeolites and advanced MOFs materials.

In conclusion, ZIF fragments were used to decorate the 12-MR of MOR directionally, causing the futile MOR to exhibit efficient propene/propane separation performances. After decoration, high kinetic selectivities of 75, 118 and 139 were achieved for ZnMOR-mIM, ZnMOR-eIM and ZnMOR-pIM, respectively. The potential of the propene/

propane separation of the resulting adsorbents has been further demonstrated by breakthrough experiments. Moreover, propene and propane uptake of the HMOR-eIM that had undergone direct ion-exchange with imidazole decreased simultaneously, showing no potential for propene/propane separation, which further verified the superiority of the strategy of using the strong interaction between zinc cations and imidazole ligands to selectively anchor imidazole in the interior of MOR. The highly efficient separation performances of the resulting adsorbents with simple synthetic processes and stable structures might potentially be applicable for industrially significant propene/propane separation. This strategy also reflected the unique advantages of the combination of traditional and new materials, which has an extensive reference value.

Acknowledgements

The work was supported by the National Key Research and Development Program of China (2016YFB0301603).

Conflict of interest

The authors declare no conflict of interest.

Keywords: gas adsorption · mordenite · propene/propane separation · ZIF fragments

How to cite: *Angew. Chem. Int. Ed.* **2020**, *59*, 6765 – 6768
Angew. Chem. **2020**, *132*, 6831 – 6834

[1] D. S. Sholl, R. P. Lively, *Nature* **2016**, *532*, 435 – 437.
[2] R. B. Eldridge, *Ind. Eng. Chem. Res.* **1993**, *32*, 2208 – 2212.
[3] a) J. Peng, H. Wang, D. H. Olson, Z. Li, J. Li, *Chem. Commun.* **2017**, *53*, 9332 – 9335; b) C. Y. Lee, Y.-S. Bae, N. C. Jeong, O. K. Farha, A. A. Sarjeant, C. L. Stern, P. Nickias, R. Q. Snurr, J. T. Hupp, S. T. Nguyen, *J. Am. Chem. Soc.* **2011**, *133*, 5228 – 5231; c) K. Li, D. H. Olson, J. Seidel, T. J. Emge, H. Gong, H. Zeng, J. Li, *J. Am. Chem. Soc.* **2009**, *131*, 10368 – 10369; d) L. Li, R.-B. Lin, X. Wang, W. Zhou, L. Jia, J. Li, B. Chen, *Chem. Eng. J.* **2018**, *354*, 977 – 982; e) H. Wang, X. Dong, V. Colombo, Q. Wang, Y. Liu, W. Liu, X.-L. Wang, X.-Y. Huang, D. M. Proserpio, A. Sironi, Y. Han, J. Li, *Adv. Mater.* **2018**, *30*, 1805088.
[4] a) P. A. Barrett, T. Boix, M. Puche, D. H. Olson, E. Jordan, H. Koller, M. A. Camblor, *Chem. Commun.* **2003**, 2114 – 2115; b) D. H. Olson, M. A. Camblor, L. A. Villaescusa, G. H. Kuehl, *Microporous Mesoporous Mater.* **2004**, *67*, 27 – 33; c) M. Palomino, A. Cantín, A. Corma, S. Leiva, F. Rey, S. Valencia, *Chem. Commun.* **2007**, 1233 – 1235; d) W. Zhu, F. Kapteijn, J. A. Moulijn, *Chem. Commun.* **1999**, 2453 – 2454; e) J. Padin, S. U. Rege, R. T. Yang, L. S. Cheng, *Chem. Eng. Sci.* **2000**, *55*, 4525 – 4535.
[5] Y. Wu, D. Yuan, D. He, J. Xing, S. Zeng, S. Xu, Y. Xu, Z. Liu, *Angew. Chem. Int. Ed.* **2019**, *58*, 10241 – 10244; *Angew. Chem.* **2019**, *131*, 10347 – 10350.
[6] a) E. F. Baxter, T. D. Bennett, C. Mellot-Draznieks, C. Gervais, F. Blanc, A. K. Cheetham, *Phys. Chem. Chem. Phys.* **2015**, *17*, 25191 – 25196; b) J. Sánchez-Laínez, A. Veiga, B. Zornoza, S. R. G. Balestra, S. Hamad, A. R. Ruiz-Salvador, S. Calero, C. Téllez, J. Coronas, *J. Mater. Chem. A* **2017**, *5*, 25601 – 25608.
[7] J. Kärger, D. M. Ruthven, D. N. Theodorou, *Diffusion in Nanoporous Materials*, Wiley, Hoboken, **2012**.
[8] a) A. R. Pradhan, J. F. Wu, S. J. Jong, W. H. Chen, T. C. Tsai, S. B. Liu, *Appl. Catal. A* **1997**, *159*, 187 – 209; b) T. He, X. Liu, S. Xu, X. Han, X. Pan, G. Hou, X. Bao, *J. Phys. Chem. C* **2016**, *120*, 22526 – 22531.
[9] a) F. Guenneau, K. Panesar, A. Nossov, M.-A. Springuel-Huet, T. Azaïs, F. Babonneau, C. Tourné-Péteilh, J.-M. Devoisselle, A. Gédéon, *Phys. Chem. Chem. Phys.* **2013**, *15*, 18805 – 18808; b) T. Azaïs, C. Tourné-Péteilh, F. Aussenac, N. Baccile, C. Coelho, J.-M. Devoisselle, F. Babonneau, *Chem. Mater.* **2006**, *18*, 6382 – 6390; c) S. Komulainen, J. Roukala, V. Zhivonitko, M. A. Javed, L. Chen, D. Holden, T. Hasell, A. Cooper, P. Lantto, V.-V. Telkki, *Chem. Sci.* **2017**, *8*, 5721 – 5727.
[10] M. Maache, A. Janin, J. C. Lavalley, E. Benazzi, *Zeolites* **1995**, *15*, 507 – 516.

Manuscript received: January 1, 2020
Accepted manuscript online: February 13, 2020
Version of record online: March 5, 2020

